cosmetics

MDPI

Article

Establishing the Inhibition of the Serine Protease Plasmin as a Skin Anti-Aging Pathway

Remo Campiche [1,*], Dominik Imfeld [1], Chennakesava Cuddapah [2], Leithe Budel [1] and Mathias Gempeler [1]

[1] dsm-firmenich, Perfumery & Beauty, Beauty & Care, 4303 Kaiseraugst, Switzerland; dominik.imfeld@dsm-firmenich.com (D.I.); leithe.budel@dsm-firmenich.com (L.B.); mathias.gempeler@dsm-firmenich.com (M.G.)
[2] Curio Biotech, 3930 Visp, Switzerland; cuddapah@curiobiotech.com
* Correspondence: remo.campiche@dsm-firmenich.com

Abstract: Plasmin is a serine protease induced by UV-irradiation in skin that contributes to inflammation. We showed that plasmin is upregulated in photo-exposed facial skin and that this correlates with increased transepidermal water loss (TEWL). Plasmin activity upregulates downstream pathways such as pro-inflammatory cytokines and matrix-metalloproteinases (MMPs). In addition, the plasminogen system modulates cutaneous melanogenesis. In this study, we investigated potential skin-aging effects of plasmin with a dual inhibitor of plasmin and its activator urokinase (uPA). We established a range of in vitro and ex vivo assays to investigate inflammation, MMP-9 activation, and collagen modulation, and the melanogenesis modulation activity of plasmin. A specific plasmin inhibitor, Amidinobenzyl Benzylsulfonyl D-Seryl Homophenylalaninamide Acetate (ABSHA), was used in these assays to downregulate these effects. We found that ABSHA was able to down-regulate UV-irradiation-induced MMP-9 expression, and subsequent collagen IV degradation, ex vivo. In addition, the increased melanin synthesis in epidermal melanocytes was reduced significantly by ABSHA. Furthermore, dermal fibroblasts treated with the plasmin inhibitor showed increased collagen I synthesis. We further investigated these effects in a two-month, monocentric, placebo-controlled human study on female Chinese volunteers. We found a significant increase in collagen density by ultrasound measurement and an increase in elasticity by cutometer assessment in the group using a formulation consisting of a 10 ppm ABSHA solution. This resulted in decreased wrinkle volumes on both the forehead and crow's feet as shown by Primos CR. Looking at age spots, there was a decrease in overall ITA° and melanin density as well as in the total age spot area. Our results establish plasmin as a skin-aging enzyme. Using specific inhibitors against plasmin shows promise against age-induced skin conditions.

Keywords: plasmin; skin; aging; Amidinobenzyl Benzylsulfonyl D-Seryl Homophenylalaninamide Acetate; tranexamic acid

Citation: Campiche, R.; Imfeld, D.; Cuddapah, C.; Budel, L.; Gempeler, M. Establishing the Inhibition of the Serine Protease Plasmin as a Skin Anti-Aging Pathway. *Cosmetics* **2024**, *11*, 103. https://doi.org/10.3390/cosmetics11030103

Academic Editor: Enzo Berardesca

Received: 23 April 2024
Revised: 27 May 2024
Accepted: 10 June 2024
Published: 19 June 2024

1. Introduction

Plasmin is a serine protease expressed as a precursor molecule called plasminogen, which, upon cleavage by the urokinase-type plasminogen activator (urokinase, uPA), becomes the active enzyme plasmin [1]. The activity of uPA is regulated by plasminogen activator inhibitors (PAI) [2]. Plasminflammation denotes a recently described systemic mechanism in which plasminogen/plasmin contribute to bradykinin-mediated inflammatory events [3]. It has been shown that tranexamic acid, an inhibitor of the conversion of plasminogen to plasmin, inhibited inflammation via, e.g., the inhibition of pro-inflammatory cytokines such as IL-1beta, IL-6, or TNFalpha in rats [4–6], corroborating the plasminflammation concept on an additional level.

Plasminogen and uPA are expressed and activated in skin cells [7–9]. More specifically, plasmin, or plasminogen, has been localized to the terminally differentiated layers of the

epidermis [10]. Expression has been shown to be elevated in photo-exposed skin such as the face, in low pigmented skin, and this correlated with increased TEWL [11–13]. In a one-month study on female Caucasian volunteers, the inhibition of plasmin and uPA by a dual inhibitor, Amidinobenzyl Benzylsulfonyl D-Seryl Homophenylalaninamide Acetate (ABSHA), showed a decrease in TEWL and thus increased skin barrier strength as elucidated by a specific tape stripping protocol, as well as reducing stinging perception [14]. In vitro, the expression and activity of both plasmin and urokinase could be upregulated by the pro-inflammatory cytokines TNFalpha and IL-1beta [15], leading to the expression of, e.g., IL-8 and CXCL5, as well as MMP-9 [14]. These effects were downregulated by ABSHA [14]. These findings provided evidence that the plasminogen/plasmin system orchestrates inflammation and associated events in the epidermis. It is thus assumed that inhibiting this plasminflammation in skin contributes significantly to the overall homeostasis and health of the skin.

Skin aging is a chronological process driven by both intrinsic and extrinsic factors [16,17]. Among the extrinsic factors, environmental triggers such as solar radiation, air pollution, and temperature were identified as contributing significantly to and accelerating intrinsically driven skin aging [18]. Visible signs of skin aging, particularly in the face, range from fine lines and deep wrinkles to loose and sagging skin with mottled hyperpigmentation or age spots [19]. On a molecular level, inflammation and oxidative stress trigger the activation of enzymes such as matrix metalloproteinases (MMPs) [20]. MMPs degrade extracellular matrix proteins such as collagens and elastic fibers [21]. More specifically, the degradation of collagen I and collagen III by MMP-1 was identified as one of the major events in skin aging leading to the formation of wrinkles [22,23]. In addition, the degradation of elastic fibers by elastases like MMP-12, neprilysin, or leukocyte-derived elastase leads to sagging skin deprived of elasticity [24,25]. Moreover, the activation of MMP-9 leads to the degradation of its main target, collagen IV [26,27]. Collagen IV is a major component of the lamina densa in the dermal–epidermal junction [28–30]. Its degradation is age-dependent and accelerated in photo-exposed skin, contributing to wrinkles and sagging [31–33]. Hence, protecting skin from the detrimental effects of MMPs or replenishing skin with extracellular matrix components is thought to slow down cutaneous age progression. As an example, hydrolyzed collagen was shown to be effective in reducing signs of skin aging such as skin dryness, laxity, and wrinkles by improving the collagen fiber structure in the dermis (reviewed in [34]).

Evidence for activities of plasmin beyond inflammation has come from studies with tranexamic acid, a uPA inhibitor, showing for example that it is able to restore collagen I loss and ameliorate wrinkles in mice suffering from dryness [35] and natural skin aging [36]. The same research group also reported that tranexamic acid increased the life span of mice, and they measured decreased blood levels of pro-inflammatory cytokines, reactive oxygen species, and MMP-9 in the presence of tranexamic acid, suggesting a role for the plasminogen system in aging [37]. Furthermore, plasmin was found to induce laminin 5 degradation and impair assembly of the basal membrane in skin-equivalents [38]. The UVA-induced degradation of collagen I and fibrillin-1 fibers in normal human fibroblasts was inhibited by tranexamic acid [39].

Tranexamic acid has also been used for the treatment of melasma, a cutaneous pigment disorder [40]. Indeed, it has been shown that the plasminogen system increased melanogenesis in skin, and that tranexamic acid was able to inhibit tyrosinase activity in human epidermal melanocytes treated with conditioned keratinocyte medium containing uPA [41].

Overall, the available data suggest plasmin to be a gateway of both inflammation and aging, making it a target for the treatment of both “plasminflammation”, as previously postulated, and “plasminaging”. In the presented study, we further investigated the cutaneous aging-related activities of plasmin and drew a link from plasminflammation to plasminaging in human skin, both in vitro and in vivo.

2. Materials and Methods

2.1. Peptide ABSHA

Origin and synthesis of peptide ABSHA, the dual inhibitor of plasmin and urokinase, is proprietary to dsm-firmenich, and was described previously by Voegeli et al. [14].

2.2. MMP-9 Upregulation and Collagen IV Degradation Ex Vivo

This experiment was conducted at Laboratoire Bio-EC, Longjumeau, France. A circular skin explant from human abdominal plastic surgery (female, Caucasian, 49 years, phototype II, with a diameter of 12 ± 1 mm) was prepared. Explants were acquired according to Declaration of Helsinki guidelines and article L.1243-4 of the French Public Health Code. Tissues were equilibrated at 37 °C in a humidified CO_2 atmosphere. Explants were cultured for seven days. On days 0 (D0), 1, 2, 5, and 6, explants were placed in Hank's Balanced Saline Solution (HBSS) and irradiated (except for non-irradiated controls) using a UV simulator RMX 3W (Vilbert Lourmat, Marne-la-Vallée, France), with 4.5 J/cm^2 UV-A corresponding to 1 minimal erythemal dose (1 MED) on a phototype II skin. At the end of irradiation, explants were again put into culture medium and further incubated. Where applicable, 2 µL (equals 2 mg/cm^2) test peptide ABSHA or vehicle (DMSO/water 50/50 *v*/*v*) was applied topically onto the explants on the same days that irradiation took place. Culture medium was half renewed on days 2 and 5. For harvesting, samples were cut in half and either formalin-fixed or frozen at −80 °C. Formalin-fixed samples were further dehydrated and impregnated in paraffin using a Leica PEARL dehydration automat. The samples were embedded using a Leica EG 1160 embedding station. Sections that were 5 µm-thick (for MMP-9 staining) were made using a Leica RM 2125 Minot-type microtome and mounted on Superfrost® histological glass slides. The frozen samples (for collagen IV staining) were cut at 7 µm thickness with a Leica CM 3050 cryostat (Leica Biosystems, Deer Park, IL, USA). The sections were then mounted on silanized glass slides (Superfrost® Plus, Fisher Scientific, Waltham, MA, USA). The microscopical observations were made using a Leica DMLB (Leica Microsystems, Wetzlar, Germany) or an Olympus BX43 or BX63 microscope (Olympus, Tokyo, Japan). Pictures were digitized with a numeric DP72 or DP74 Olympus camera with CellSens storing software version 4.1 (Evident Corp., Tokyo, Japan).

The cell viability of the epidermal and dermal structures was monitored on formalin-fixed paraffin-embedded (FFPE) skin sections following Masson's trichrome staining procedure, Goldner variant. Viability was assessed by microscopy. MMP-9 immunostaining was carried out on FFPE skin sections with a polyclonal rabbit anti-human MMP-9 antibody (Novus Biologicals, Minneapolis, MN, USA, reference NB600-1217) diluted at 1:50 in PBS–BSA 0.3%, incubated over night at room temperature, using Vectastain Kit Vector amplifier system avidin/biotin, and revealed by VIP (Vector laboratories, Newark, CA, USA, reference SK-4600), a substrate of peroxidase giving a violet staining. Collagen IV immunostaining was carried out on frozen skin sections with a monoclonal mouse anti-human collagen IV antibody (DAKO, Santa Clara, CA, USA, ref. M0785, clone CIV22) diluted at 1:25 in PBS, BSA 0.3%, and Tween 20 (0.05%) for 1 h at room temperature, and revealed by a goat anti-mouse secondary antibody AF488 (Lifetechnologies, Carlsbad, CA, USA, reference A11001). The staining was performed manually and assessed by microscopical observation. Image analysis for both MMP-9 and collagen IV quantification was performed on n = 9 images per test condition, using CellSens software version 4.1 (Evident Corp. Tokyo, Japan).

2.3. Collagen I In Vitro Assay

Normal human dermal fibroblasts (NHDF, from CELLnTEC advanced cell systems, Bern, Switzerland, Caucasian female donor, age 26, isolated from breast) were seeded in 96-well culture plates at 40,000 cells/well in Dulbecco's modified Eagle's medium (DMEM, high-glucose, 1% fetal bovine serum) (VWR, reference 392-0416) for 5–7 h. They were then starved in Dulbecco's modified Eagle's medium (DMEM, low-glucose, 1% fetal bovine serum) (VWR, Dietikon, Switzerland, reference 392-0407) overnight. Twenty-four hours

after seeding fresh Dulbecco's modified Eagle's medium (DMEM, low-glucose, 1% fetal bovine serum) (VWR Dietikon, Switzerland, reference 392-0407) was added containing ABSHA. A control (vehicle medium only) and positive control (Recombinant Human TGF-β1, PeproTech, London, UK, reference 100-21, at 10 ng/mL) were included as well for analysis and assay verification purposes. The cells were exposed to the treatment for 72 h in a humidified incubator at 37 °C and 5% CO_2. After washing and detaching the cells, intracellular collagen I was stained using a monoclonal mouse anti-human collagen I antibody (Novus Biologicals, Minneapolis, MN, USA, reference NB600-450), and detected by an Alexa Fluor 647 secondary antibody (Thermo Fisher Scientific, Waltham, MA, USA, reference A21235). Cells were analyzed in an Attune NxT Flow Cytometer (Thermo Fisher Scientific, Waltham, MA, USA) (Figure S1). To better illustrate the results, we converted the data obtained as flow cytometer diagrams to bar graphs as follows: the fluorescence value of the number of differences between cell number and the active of interest versus the cell number of the control were normalized. This way, a potential effect on proliferation by the active is normalized and only the total collagen levels per cell is represented. The control was then set to 100% and the samples were adjusted accordingly.

2.4. Melanin Assay in Human Epidermal Melanocytes

Human epidermal melanocytes (HEMs) were obtained from abdominal plastic surgery, from a female donor with phototype III-IV (slightly colored). The HEMs were seeded in supplemented melanocyte growth medium (Curio Biotech, Visp, Switzerland, reference CB-MC-GM) containing 2% FBS and were grown for 1 day in a humidified CO_2 incubator at 37 °C. After 1 day of culture, cells were treated with plasmin (Sigma Aldrich, Burlington, MA, USA) reference P1867 with 3.6 u/mg protein) and/or test compounds for 2 days. After 2 days, cells were pelleted and replicate condition tubes were photographed, then the cells were subjected to melanin extraction and quantified in a multimode plate reader (Hidex Sense, Turku, Finland) at 405 nm wavelength. For melanin extraction, cells were subjected to melanin extraction in 1M NaOH solution that was heated for 95 °C for 30 min; supernatants were centrifuged, and melanin was quantified in a microplate reader using synthetic melanin as standard (Sigma-Aldrich, Burlington, MA, USA, reference M8631).

2.5. Tyrosinase Assay

HEMs were seeded in supplemented melanocyte growth medium (Curio Biotech, reference CB-MC-GM) containing 2% FBS for 1 day. They were then treated with the 2 μg/mL plasmin and test compounds for a further 2 days. First, the cells were lysed in mammalian cell lysis buffer (Sigma-Aldrich, reference C2798) and total protein concentration was determined through BCA (Bicinchoninic Acid) assay (Sigma-Aldrich, Burlington, MA, USA, reference 71285-M). Briefly, 50 μL of each sample was added to 200 μL of BCA reagent in a microplate and incubated for 30 min at 37 °C. Absorbance was measured at 592 nm in a microplate reader (Hidex Sense, Turku, Finland). Concentration was determined using a calibration curve with BSA standards. An equal amount of protein was loaded on a 96-well plate and 10 mM of L-DOPA (3-(3,4-Dihydroxyphenyl-2,5,6-d3)-L-alanine) was added. Tyrosinase activity was detected over the time taken to convert L-DOPA to DOPAquinone. As soon as L-DOPA was added at time zero, absorbance readings were taken in a microplate reader (Hidex Sense, Turku, Finland) at 405 nm wavelength. Further readings were taken until a clear signal was detected. Tyrosinase activity was calculated comparing the readings with the zero time point. At each time point, the blank values were subtracted. The assay was performed in triplicate. Results were presented in percentages compared to the untreated control with mean ± SEM.

2.6. Human Study

We conducted a monocentric, placebo-controlled, and randomized study in the city of Guangzhou, People's Republic of China. The study took place from 15 March 2023 to 17 May 2023. The study was formally approved by the Ethics Committee of Guangdong

Daily Chemical Industry (approval number GDIRB (2023)3-2) prior to initiation of the study. The study took place according to the Helsinki principle and subjects gave their written informed consent to participate. They could withdraw their consent at any time without reason. The subjects were healthy female Chinese volunteers, aged from 40 to 65 years with skin phototype I–III according to the Fitzpatrick scale, with visible wrinkles on the forehead and crow's feet and at least one obvious age spot with an ITA° difference greater than 10° from the surrounding skin and a diameter of less than 3 mm. Otherwise, standard inclusion and exclusion criteria were applied. Adverse effects were monitored. A total of 34 subjects in the placebo group and 34 subjects in the active formulation group completed the study. The volunteers applied their respective formulation (about 1 g at the size of a hazelnut, Supplementary Table S1) on the full face twice daily—in the morning and in the evening—continuously for 56 days. This study contained a wash-out phase of 7 days during which all subjects used the placebo formulation twice daily on the full face. Measurements were taken in a controlled environment of 21 ± 1 °C and 50 ± 5% relative humidity.

Instrumental Measurements in the Human Study

TEWL was measured using a TEWAmeter Hex (Courage & Khazaka, Cologne, Germany). We measured on five selected facial sites (Figure S4) according to the facial color map outline described previously [42]. Each measurement was taken at each timepoint, in triplicate. Dermal thickness was measured by ultrasound using a DermaLab® Combo device (Cortex Technology, Aalborg, Denmark). Dermal thickness was measured on the crow's feet and the cheek (Figure S5). Elasticity was measured using a Cutometer MPA580 device (Courage & Khazaka, Cologne, Germany), also in triplicate at both the crow's feet and the cheek area (Figure S5). Wrinkles were measured on the forehead and on the crow's feet area (Figure S5) using a Primos CR device (Canfield, Parsippany, NJ, USA). The average of three measurements was recorded. To monitor the effect of the plasmin inhibitor on age spots, we selected one prominent age spot per volunteer as described in the inclusion criteria. We measured the ITA° of the spot with a spectrophotometer CM-26d (Konica Minolta, Tokyo, Japan). The average of 3 measurements per site was recorded. To calculate the spot/area ratio, we took full face images of the selected spot and its surrounding area with a VISIA CR (Canfield, Parsippany, NJ, USA) and calculated the ratio with Image Pro Plus software version 7.0 (MediaCybernetics, Rockville, MD, USA). At timepoints D14, D28, and D56, the volunteers filled in a self-assessment questionnaire using a nine-point scale where 1 meant strongly disagree with the statement and 9 meant strongly agree with the statement. Scores of six and higher were considered positive/affirmative answers.

3. Results

3.1. MMP-9 Protein Expression and Collagen IV Degradation Ex Vivo

To investigate the effect of plasmin on the functional effects of MMP-9 expression ex vivo, we induced MMP-9 by UV-irradiation in skin tissue and monitored both the MMP-9 expression and collagen IV degradation. We showed that MMP-9 is increased by UV-irradiation in skin explants by 2.18-fold. Adding ABSHA inhibited the expression of MMP-9 to 1.39-fold (Figure 1a), which is visible in the staining of the explants (Figure 1b). To see whether this has an impact on the downstream targets of MMP-9, we investigated collagen IV expression in UV-irradiated skin explants. We found a significant reduction of total collagen IV by 17% ($p < 0.05$). In the presence of the inhibitor peptide ABSHA, this downregulation was almost completely inhibited (Figure 1c), which is also seen in the staining of the explants (Figure 1d).

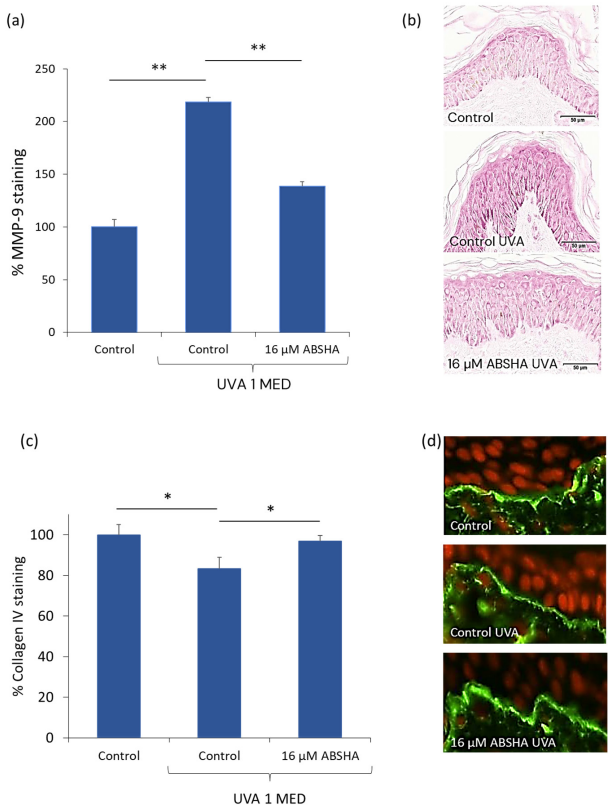

Figure 1. MMP-9 and collagen IV protein quantification in UV-irradiated skin ex vivo. (**a**) Quantification of MMP-9 staining. (**b**) Representative images of MMP-9 staining in skin sections. Note the darker red staining in the control sample irradiated with UVA. (**c**) Quantification of collagen IV staining in skin explants. (**d**) Representative images of collagen IV staining (green fluorescence) in skin sections counterstained for nuclei (red fluorescence). * $p < 0.05$, ** $p < 0.01$ by paired *t*-test, error bars represent standard error of the mean of $n = 9$ per treatment.

3.2. Collagen I Expression in Human Dermal Fibroblasts

Since we could confirm the impact of the plasminogen pathway on collagen IV degradation (Figure 1), we were interested in whether it modulated other cutaneous collagens. We therefore investigated collagen I expression in dermal fibroblasts. Indeed, we found a significant and dose-responsive 1.8-fold ($p < 0.05$) increase in collagen I expression in dermal fibroblasts treated with ABSHA (Figure 2).

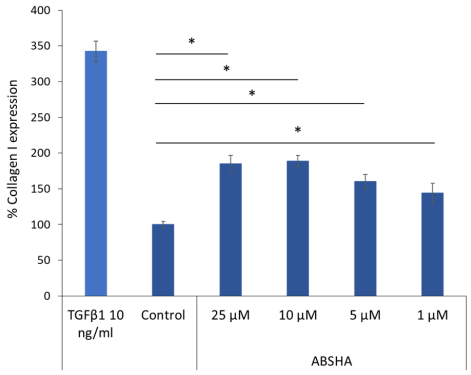

Figure 2. Collagen I expression in dermal fibroblasts. Dermal fibroblasts were treated with ABSHA. Immunostaining of collagen I was analyzed by flow cytometry. * $p < 0.05$ by unpaired *t*-test. Error bars represent standard error of the mean of $n = 4$ per treatment.

3.3. Modulation of Melanogenesis by the Plasminogen Pathway and Its Inhibitors

We were able to induce the intracellular melanin content of normal human epidermal melanocytes via plasmin exposure (Figure S2). Based on several experiments, we found a concentration of 2 µg/mL plasmin in our assay to yield the most robust and reproducible result. We also found a dose-responsive inhibition of this melanin increase through the addition of the plasmin inhibitor ABSHA (Figure S3). Comparing the activity of plasmin and the plasminogen inhibitors ABSHA and tranexamic acid, we found a reduction in intracellular melanin in the presence of ABSHA (−58%, $p < 0.05$) and tranexamic acid (−16%) (Figure 3a). Interestingly, we also found a reduction in melanin content without the stimulation of plasmin (Figure 3a).

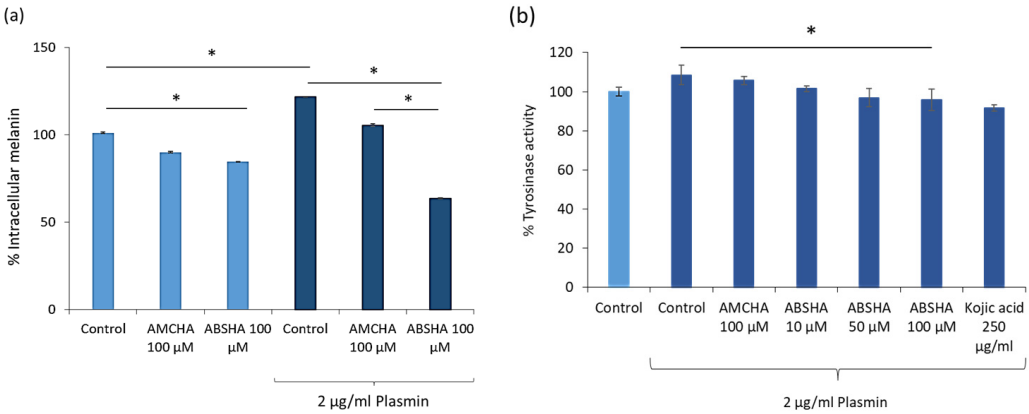

Figure 3. Suppression of melanogenesis by plasmin inhibition. (**a**) Quantification of intracellular melanin in epidermal melanocytes treated without and with plasmin and inhibitors. (**b**) Tyrosinase activity without and with plasmin and inhibitors. Kojic acid served as positive control for melanogenesis modulation, and AMCHA served as a reference substance and known inhibitor of the plasmin/plasminogen system. AMCHA = tranexamic acid. * $p < 0.05$ by paired *t*-test. Error bars represent standard error of the mean of $n = 3$ per treatment.

3.4. Tyrosinase Modulation by Plasmin and Its Inhibitors

As plasmin induced melanin synthesis in NHEM, we were interested in the effect of plasmin and its inhibitors on tyrosinase activity. We found a slight but non-significant increase in tyrosinase activity in the presence of plasmin (Figure 3b). This increase in tyrosinase activity could be suppressed by the addition of the plasmin inhibitor ABSHA and reached significance (−12%, $p < 0.05$) at 100 µM (Figure 3b).

3.5. TEWL Is Significantly Decreased by ABSHA In Vivo

To have a proof-of-concept and positive control in the human study, we measured the TEWL at the five facial sites shown in Figure S4. On each site, we recorded a time-dependent decrease in the TEWL in the group using the active formulation while the TEWL in the placebo group only slightly changed over time. The combined TEWL over all five measurement sites went down significantly compared to day 0 in the group using the 10 ppm ABSHA formulation, namely −1.10 at day 14, −1.99 at day 28, and −2.66 at day 56 (Figure 4). These measurements were all markedly different to the placebo group where the changes over time were −0.23 at day 14, −0.31 at day 28, and −0.36 at day 56 (all $p < 0.001$ between groups (Figure 4)).

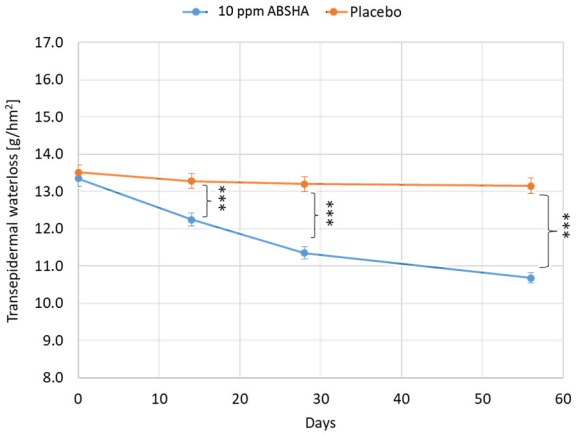

Figure 4. Transepidermal water loss (TEWL) in the face. Graph representing the evolution of the TEWL of all five sites (Figure S3) combined during the in vivo study. *** $p < 0.001$ by Mann–Whitney U test. Error bars represent standard error of the mean of $n = 170$ per treatment.

3.6. Dermal Intensity Increased over Time on the Cheeks and the Crow's Feet

We measured the dermal intensity by ultrasound and found a steady and significant increase in the signal (echogenicity) over time in the group using the 10 ppm ABSHA formulation, while the signal stayed constant in the placebo group for both facial sites (Figure 5). The difference in the ultrasound signal was significantly different already at day 14 on the cheek ($p < 0.01$) (Figure 5a), while it became significant vs the placebo on day 28 ($p < 0.01$) in the crow's feet area (Figure 5b).

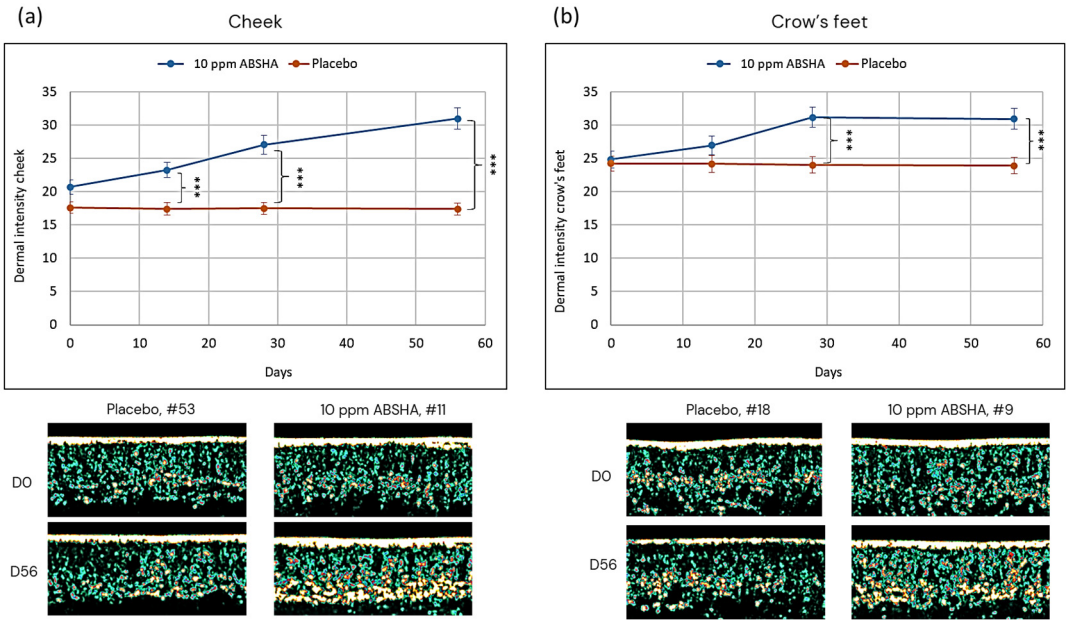

Figure 5. Evolution of dermal intensity on (**a**) the cheek and (**b**) the crow's feet. Images show representative skin sections. Areas of high intensity are from bright yellow to white. Areas of low intensity are from green to black. *** $p < 0.001$ by Mann–Whitney U test. Error bars represent standard error of the mean of $n = 34$ per treatment.

3.7. Elasticity Improved in the Group Using the 10 ppm ABSHA Formulation

Elasticity was measured on the cheeks and the crow's feet area. We observed a steady increase in the R2 value (gross elasticity after strain) which was significant at all timepoints, D14 ($p < 0.05$), D28, and D56 (both $p < 0.001$), compared to the placebo group (Figure 6). This result was obtained at both the cheek and the crow's feet area. It reached a delta

between the active formulation and placebo at D56 of 0.096 for the cheek and of 0.1 for the crow's feet area.

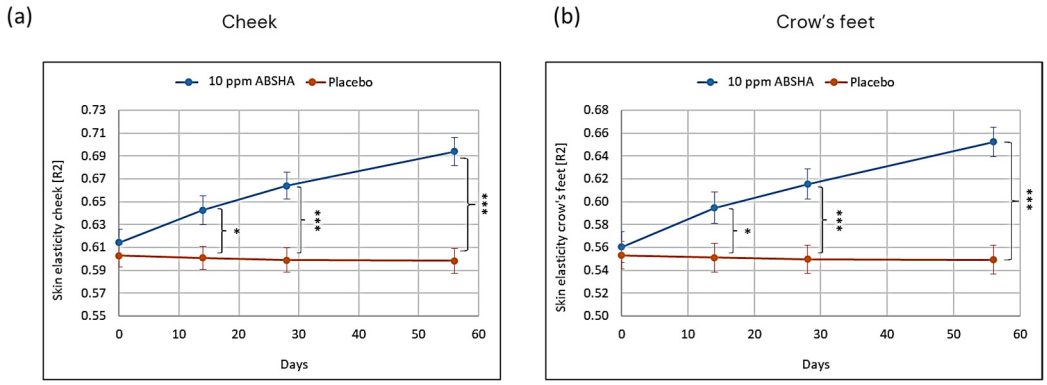

Figure 6. Evolution of elasticity (R2) over time on (**a**) the cheek and (**b**) the crow's feet. * $p < 0.05$, *** $p < 0.001$ by Mann–Whitney U test. Error bars represent standard error of the mean of $n = 34$ per treatment.

3.8. Less Wrinkle Volume over Time

Since the dermal ultrasound value, indicative of an increase in collagen density, increased in the active formulation group, we expected an improvement for wrinkles. Measuring the wrinkle volume revealed an improvement in wrinkles on the forehead (Figure 7a) and on the crow's feet (Figure 7b). We measured a steady decrease in wrinkle volume on the forehead of up to -0.71 mm^3 for the 10 ppm ABSHA group, while it stayed the same in the placebo group (0.07 mm^3 at day 56). The difference between the placebo and active group was significant at all timepoints. For the crow's feet area, we measured a decrease in wrinkle volume of up to -0.46 mm^3 at day 56 in the ABSHA group compared to 0.03 mm^3 in the placebo group. These differences were also significant between the active formulation group and the placebo group at all timepoints. Figure 7 shows Primos-derived images of a selected volunteer, each with a visibly improved wrinkle profile at day 56 compared to day 0.

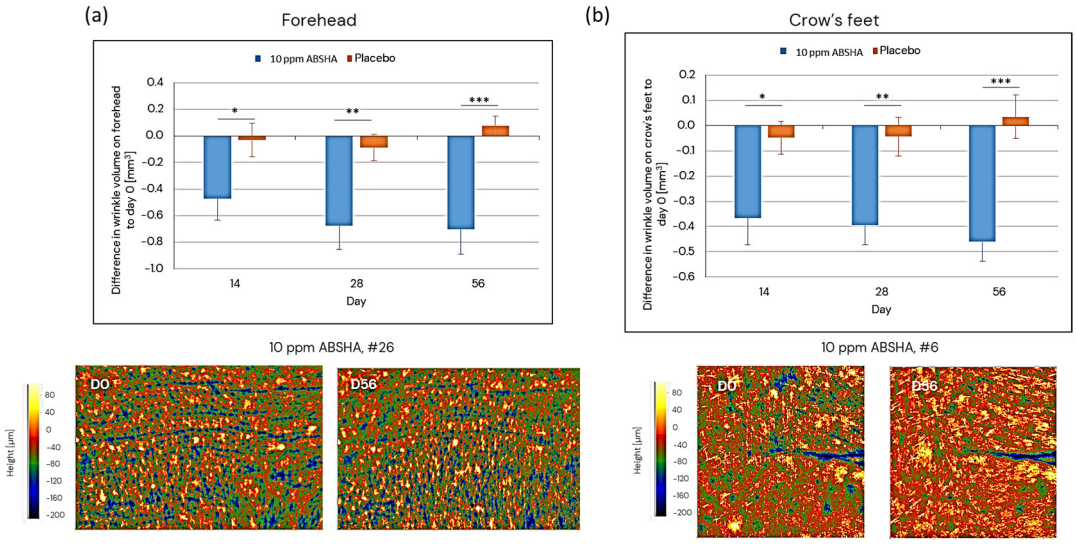

Figure 7. Evolution of wrinkle volume on (**a**) the forehead and (**b**) the crow's feet. Images show Primos scans of the forehead and crow's feet areas of a distinct volunteer at the baseline (D0) and end of the study (D56). Colors represent different depths (blue) and heights (yellow) over the plane (orange). * $p < 0.05$, ** $p < 0.01$, *** $p < 0.001$ by Man–Whitney U test. Error bars represent standard error of the mean of $n = 34$ per treatment.

3.9. Modulation of Age Spots by a 10 ppm ABSHA Formulation

We monitored a distinct age spot in each volunteer. We observed a time-dependent increase in the ITA° value in the group using the active formulation, meaning the spot became lighter, while the values slightly decreased in the placebo group (Figure S6a). The increase seen with the active formulation was significant versus the baseline for all timepoints, but not significant versus the placebo group. However, looking at the delta values at each timepoint versus D0, it became significant versus the placebo at all timepoints (Figure 8a). When calculating the spot/area ratio, we found a steady decrease in the ratio for the active formulation group, meaning the spot became smaller compared to the measured area, while there was a steady increase in the ratio in the placebo group (Figure S6b), and the values of the two groups were significantly different at D28 and D56 ($p < 0.01$ and $p < 0.001$, respectively). Furthermore, the delta values to the baseline differed significantly between the placebo and active formulation groups at all timepoints (Figure 8b). Figure 8c depicts an example age spot in a volunteer, highlighting the visual effect of the active formulation.

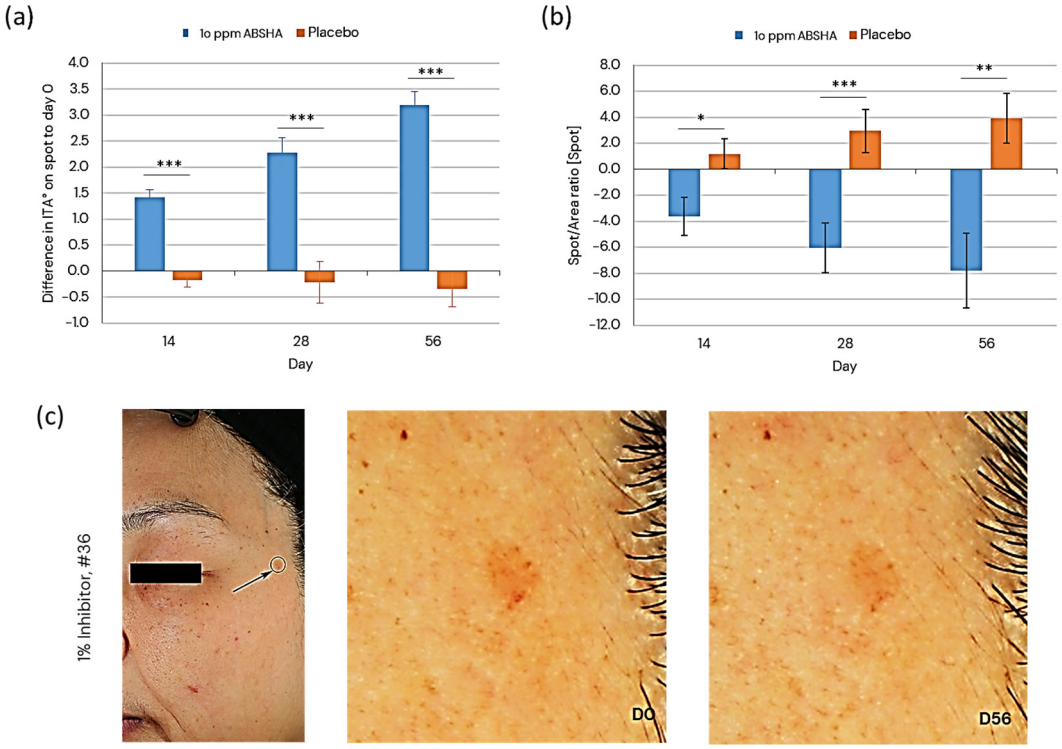

Figure 8. Evolution of (**a**) age spot color and (**b**) age spot size. Images in (**c**) show the location of a particular age spot and its color evolution from the baseline (D0) to the end of the study (D56) when treated with the 10 ppm ABSHA formulation. * $p < 0.05$, ** $p < 0.01$, *** $p < 0.001$ by Mann–Whitney U test. Error bars represent standard error of the mean of $n = 34$ per treatment.

3.10. Self-Assessment Questionnaire

The volunteers filled in a self-assessment questionnaire at D14, D28, and D56, answering whether they had experienced an improvement in their facial aging signs during the study. Already at D14 we found significant differences between the placebo and the active formulation group which remained until D56 (Figure 9).

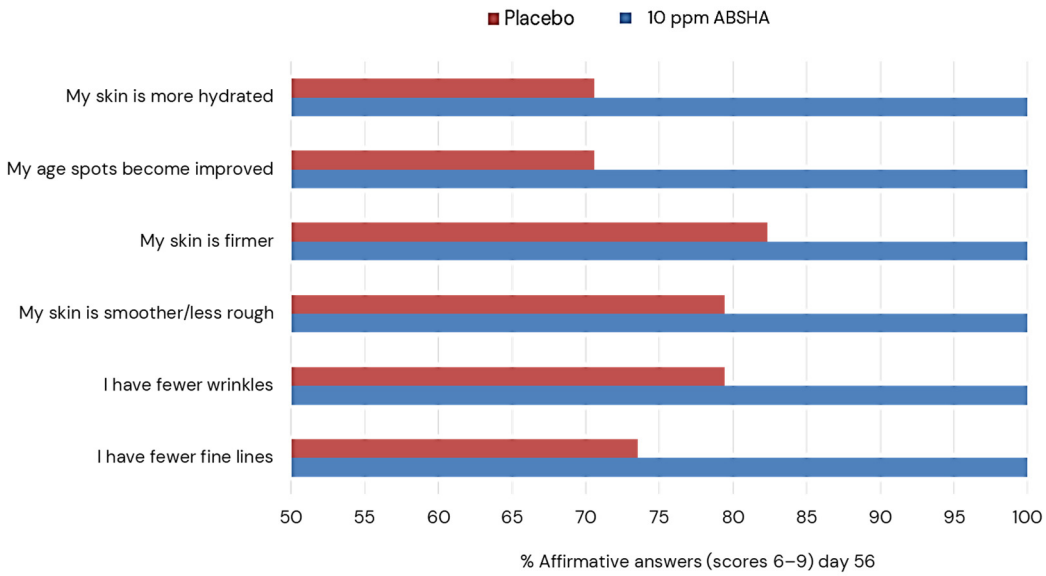

Figure 9. Self-assessment questionnaire. Shown are the cumulative affirmative answers corresponding to a score of 6 or higher for each question at the end of the study (day 56). All group comparisons of placebo vs active formulations are significant ($p < 0.001$ by Mann–Whitney U test).

4. Discussion

The serine protease plasmin has been established as a key enzyme in regulating inflammatory events related to skin barrier integrity and skin dryness [14]. Previous work on other plasmin inhibitors suggested activities of this protease beyond inflammation, such as collagen degradation and melanin synthesis [38,39,41]. To investigate such activities of plasmin in skin and to establish this enzyme as part of a skin aging pathway, we conducted a range of in vitro, ex vivo, and in vivo studies using our proprietary plasmin inhibitor ABSHA. Consistent with previous work using a different plasmin inhibitor, tranexamic acid, we found potential anti-aging activities in vitro and ex vivo (Figures 1–3). Differently from tranexamic acid, ABSHA is a dual inhibitor of both plasmin and its activator uPA [14]. This might explain why ABSHA was superior to tranexamic acid in a melanin assay on human melanocytes (Figure 3a). Our finding that the activation of plasmin induces MMP-9, which in turn degrades collagen IV (Figure 1), adds to the previous finding that plasmin activation degrades laminin in the skin's basal membrane [38] and further corroborates its contribution to skin aging on a molecular level. This finding also showed that, by inhibiting plasmin, we can inhibit the downstream collagen IV degradation pathway.

This study extends previous knowledge with a human study where we were able to measure skin anti-aging effects in a cohort of Chinese female volunteers, applying a 10 ppm solution of the plasmin inhibitor ABSHA for two months. We measured the TEWL as proof of concept and to monitor the proper activity of the formulation containing the plasmin inhibitor (Figure 4). Dry skin has been reported to occur frequently in older individuals, due, for example, to hormone decline leading to decreased water retention in the stratum corneum [43]. Improvement of the TEWL in the group using the active formulation was in line with previous findings and reports showing plasmin's correlation with an impaired skin barrier and hydration [12]. It could also be seen as an anti-aging effect of the plasmin inhibitor. In line with our in vitro and ex vivo findings, we could show an improvement of skin aging signs such as wrinkles (Figure 7) and elasticity (Figure 6), which depend on an intact extracellular matrix. Intriguingly, we could show by ultrasound that the dermal density (echogenicity), indicative of more proteins (collagen or elastin) [44], was increased in the active group (Figure 5). Our findings further corroborate previous work showing that plasmin and MMPs cause damage to the basement membrane [45] and that inhibiting plasmin has beneficial effects on tissue collagen content. Furthermore, age spots were positively affected by plasmin inhibition (Figure 8). Similarly, plasmin-like activity

correlated significantly with darker solar lentigo and skin tone in a study with Japanese men [46]. A limitation of our in vivo data may be that it was collected purely non-invasively. Therefore, our conclusions on collagen synthesis and melanin inhibition in vivo are based on extrapolation from the in vitro data presented herein and accepted knowledge of the employed methods. Looking at molecular changes in biopsies or tape strips would further elucidate the activity of plasmin and its inhibitor in vivo. In addition, we did not measure plasmin activity itself in the in vivo study here. However, based on previously published data showing enhanced plasmin activity in the face as compared to photo protected skin areas [11,13], we can assume that, since we measured facial parameters, we have significant plasmin activity present in our volunteers. Furthermore, as the inhibitor used is rather specific for plasmin and its activator, we conclude that the in vivo effects seen in this study are due to the inhibition of the plasmin pathway.

In summary, by using a dual inhibitor of the serine protease plasmin and its activator uPA, we establish plasmin and its downstream targets as a skin aging pathway. Inhibiting this pathway not only targets plasminflammation but extends its activity towards plasminaging. Our data provide evidence that inhibiting plasmin with the inhibitor ABSHA results in skin care benefits spanning from the outermost layers of the skin down to the dermis.

Supplementary Materials: The following supporting information can be downloaded at: https://www.mdpi.com/article/10.3390/cosmetics11030103/s1, Figure S1. Flow cytometer diagrams (scatter plots) for collagen I expression in dermal fibroblasts after compound treatment; Figure S2. Dose responsive stimulation of intracellular melanin content with plasmin in epidermal melanocytes; Figure S3. Dose responsive inhibition of plasmin stimulated intracellular melanin content by the plasmin inhibitor ABSHA in epidermal melanocytes; Figure S4. Transepidermal water loss (TEWL) in the face; Figure S5. Areas used for anti-aging measurements; Figure S6. Evolution of (a) age spot color ITA° values and (b) age spot size by spot to area ratio; Table S1. Composition of formulations used in in vivo study.

Author Contributions: Conceptualization, R.C. and M.G.; methodology, R.C., D.I., C.C. and L.B.; validation, R.C. and M.G.; formal analysis, R.C., D.I., C.C. and L.B.; investigation, R.C., D.I., C.C. and L.B.; resources, R.C. and M.G.; data curation, R.C., D.I., C.C. and L.B.; writing—original draft preparation, R.C.; writing—review and editing, D.I., C.C. and M.G.; supervision, M.G.; project administration, R.C.; funding acquisition, M.G. All authors have read and agreed to the published version of the manuscript.

Funding: This research received no external funding.

Institutional Review Board Statement: The in vivo study was formally approved by the Ethics Committee of Guangdong Daily Chemical Industry (approval number GDIRB (2023)3-2) prior to initiation of the study. The study took place according to the Helsinki principle and subjects gave their written informed consent to participate. They could withdraw their consent at any time without reason.

Informed Consent Statement: Informed consent was obtained from all subjects involved in the study. They could withdraw their consent at any time without reason.

Data Availability Statement: Data is contained within the article or Supplementary Materials.

Acknowledgments: We are grateful to the donors of the explants and the volunteers in the in vivo study for their participation. We would like to thank Clarissa Stoll, Anson Zhang, Eve Chen (all dsm-firmenich), Roberto Salvi (Curio Biotech), and the staff at Laboratoire Bio-EC and Landproof test institute for expert technical assistance in this study.

Conflicts of Interest: The peptide ABSHA mentioned in this study is marketed by dsm-firmenich under the trade name SYN-UP®. The sequence is patent protected by WO2009026949 and WO2014009862. The authors R.C., D.I., L.B., and M.G. are employees of dsm-firmenich and received regular salaries from this company. C.C. is an employee of Curio Biotech and received a regular salary from this company. This study was funded by dsm-firmenich. No other conflicts are to be declared. Part of this

work was presented as a poster at SCC76 2022 in Los Angeles, and as a podium presentation at the Cosmetic Science Conference 2023 in Berlin.

References

1. Kramer, M.D.; Schaefer, B.M.; Reinartz, J. Plasminogen Activation by Human Keratinocytes: Molecular Pathways and Cell-Biological Consequences. *Biol. Chem. Hoppe-Seyler* **1995**, *376*, 131–141.
2. Sillen, M.; Declerck, P.J. A Narrative Review on Plasminogen Activator Inhibitor-1 and Its (Patho)Physiological Role: To Target or Not to Target? *Int. J. Mol. Sci.* **2021**, *22*, 2721. [CrossRef]
3. Maas, C. Plasminflammation-An Emerging Pathway to Bradykinin Production. *Front. Immunol.* **2019**, *10*, 2046. [CrossRef]
4. Walker, P.F.; Foster, A.D.; Rothberg, P.A.; Davis, T.A.; Bradley, M.J. Tranexamic acid decreases rodent hemorrhagic shock-induced inflammation with mixed end-organ effects. *PLoS ONE* **2018**, *13*, e0208249. [CrossRef]
5. Teng, Y.; Feng, C.; Liu, Y.; Jin, H.; Gao, Y.; Li, T. Anti-inflammatory effect of tranexamic acid against trauma-hemorrhagic shock-induced acute lung injury in rats. *Exp. Anim.* **2018**, *67*, 313–320. [CrossRef]
6. Prudovsky, I.; Kacer, D.; Zucco, V.V.; Palmeri, M.; Falank, C.; Kramer, R.; Carter, D.; Rappold, J. Tranexamic acid: Beyond antifibrinolysis. *Transfusion* **2022**, *62* (Suppl. S1), S301–S312. [CrossRef]
7. Rotem, N.; Axelrod, J.H.; Miskin, R. Induction of urokinase-type plasminogen activator by UV light in human fetal fibroblasts is mediated through a UV-induced secreted protein. *Mol. Cell Biol.* **1987**, *7*, 622–631.
8. Marschall, C.; Lengyel, E.; Nobutoh, T.; Braungart, E.; Douwes, K.; Simon, A.; Magdolen, V.; Reuning, U.; Degitz, K. UVB increases urokinase-type plasminogen activator receptor (uPAR) expression. *J. Investig. Dermatol.* **1999**, *113*, 69–76. [CrossRef]
9. Hashimoto, K.; Singer, K.H.; Lide, W.B.; Shafran, K.; Webber, P.; Morioka, S.; Lazarus, G.S. Plasminogen activator in cultured human epidermal cells. *J. Investig. Dermatol.* **1983**, *81*, 424–429. [CrossRef]
10. Voegeli, R.; Rawlings, A.V.; Haftek, M. Expression and ultrastructural localization of plasmin(ogen) in the terminally differentiated layers of normal human epidermis. *Int. J. Cosmet. Sci.* **2019**, *41*, 624–628. [CrossRef]
11. Voegeli, R.; Rawlings, A.V.; Doppler, S.; Heiland, J.; Schreier, T. Profiling of serine protease activities in human stratum corneum and detection of a stratum corneum tryptase-like enzyme. *Int. J. Cosmet. Sci.* **2007**, *29*, 191–200. [CrossRef]
12. Voegeli, R.; Rawlings, A.V.; Doppler, S.; Schreier, T. Increased basal transepidermal water loss leads to elevation of some but not all stratum corneum serine proteases. *Int. J. Cosmet. Sci.* **2008**, *30*, 435–442. [CrossRef]
13. Raj, N.; Voegeli, R.; Rawlings, A.V.; Summers, B.; Munday, M.R.; Lane, M.E. Variation in the activities of late stage filaggrin processing enzymes, calpain-1 and bleomycin hydrolase, together with pyrrolidone carboxylic acid levels, corneocyte phenotypes and plasmin activities in non-sun exposed and sun-exposed facial stratum corneum of different ethnicities. *Int. J. Cosmet. Sci.* **2016**, *38*, 567–575.
14. Voegeli, R.; Wikstroem, P.; Campiche, R.; Steinmetzer, T.; Jackson, E.; Gempeler, M.; Imfeld, D.; Rawlings, A.V. The effects of benzylsulfonyl-D-Ser-homoPhe-(4-amidino-benzylamide), a dual plasmin and urokinase inhibitor, on facial skin barrier function in subjects with sensitive skin. *Int. J. Cosmet. Sci.* **2017**, *39*, 109–120. [CrossRef]
15. Bechtel, M.J.; Reinartz, J.; Rox, J.M.; Inndorf, S.; Schaefer, B.M.; Kramer, M.D. Upregulation of Cell-Surface-Associated Plasminogen Activation in Cultured Keratinocytes by Interleukin-1b and Tumor Necrosis Factor-a. *Exp. Cell Res.* **1996**, *223*, 395–404. [CrossRef]
16. Farage, M.A.; Miller, K.W.; Elsner, P.; Maibach, H.I. Intrinsic and extrinsic factors in skin ageing: A review. *Int. J. Cosmet. Sci.* **2008**, *30*, 87–95. [CrossRef]
17. Farage, M.A.; Miller, K.W.; Elsner, P.; Maibach, H.I. Characteristics of the Aging Skin. *Adv. Wound Care (New Rochelle)* **2013**, *2*, 5–10. [CrossRef]
18. Krutmann, J.; Bouloc, A.; Sore, G.; Bernard, B.A.; Passeron, T. The skin aging exposome. *J. Dermatol. Sci.* **2017**, *85*, 152–161. [CrossRef]
19. Trojahn, C.; Dobos, G.; Lichterfeld, A.; Blume-Peytavi, U.; Kottner, J. Characterizing facial skin ageing in humans: Disentangling extrinsic from intrinsic biological phenomena. *Biomed. Res. Int.* **2015**, *2015*, 318586. [CrossRef]
20. Tigges, J.; Krutmann, J.; Fritsche, E.; Haendeler, J.; Schaal, H.; Fischer, J.W.; Kalfalah, F.; Reinke, H.; Reifenberger, G.; Stuhler, K.; et al. The hallmarks of fibroblast ageing. *Mech. Ageing Dev.* **2014**, *138*, 26–44. [CrossRef]
21. Quan, T.; Qin, Z.; Xia, W.; Shao, Y.; Voorhees, J.J.; Fisher, G.J. Matrix-degrading metalloproteinases in photoaging. *J. Investig. Dermatol. Symp. Proc.* **2009**, *14*, 20–24. [CrossRef]
22. Brennan, M.; Bhatti, H.; Nerusu, K.C.; Bhagavathula, N.; Kang, S.; Fisher, G.J.; Varani, J.; Voorhees, J.J. Matrix metalloproteinase-1 is the major collagenolytic enzyme responsible for collagen damage in UV-irradiated human skin. *Photochem. Photobiol.* **2003**, *78*, 43–48. [CrossRef]
23. Agren, M.S.; Schnabel, R.; Christensen, L.H.; Mirastschijski, U. Tumor necrosis factor-α-accelerated degradation of type I collagen in human skin is associated with elevated matrix metalloproteinase (MMP)-1 and MMP-3 ex vivo. *Eur. J. Cell Biol.* **2015**, *94*, 12–21. [CrossRef]
24. Imokawa, G.; Ishida, K. Biological mechanisms underlying the ultraviolet radiation-induced formation of skin wrinkling and sagging I: Reduced skin elasticity, highly associated with enhanced dermal elastase activity, triggers wrinkling and sagging. *Int. J. Mol. Sci.* **2015**, *16*, 7753–7775. [CrossRef]

25. Imokawa, G.; Nakajima, H.; Ishida, K. Biological mechanisms underlying the ultraviolet radiation-induced formation of skin wrinkling and sagging II: Over-expression of neprilysin plays an essential role. *Int. J. Mol. Sci.* **2015**, *16*, 7776–7795. [CrossRef]
26. Oikarinen, A.; Kylmaniemi, M.; Autio-Harmainen, H.; Autio, P.; Salo, T. Demonstration of 72-kDa and 92-kDa forms of type IV collagenase in human skin: Variable expression in various blistering diseases, induction during re-epithelialization, and decrease by topical glucocorticoids. *J. Investig. Dermatol.* **1993**, *101*, 205–210. [CrossRef]
27. Gschwandtner, M.; Purwar, R.; Wittmann, M.; Baumer, W.; Kietzmann, M.; Werfel, T.; Gutzmer, R. Histamine upregulates keratinocyte MMP-9 production via the histamine H1 receptor. *J. Investig. Dermatol.* **2008**, *128*, 2783–2791. [CrossRef]
28. Sage, H. Collagens of Basement Membranes. *J. Investig. Dermatol.* **1982**, *79*, 51–59. [CrossRef]
29. Theocharidis, G.; Connelly, J.T. Minor collagens of the skin with not so minor functions. *J. Anat.* **2019**, *235*, 418–429. [CrossRef]
30. Hasegawa, H.; Naito, I.; Nakano, K.; Momota, R.; Nishida, K.; Taguchi, T.; Sado, Y.; Ninomiya, Y.; Ohtsuka, A. The distributions of type IV collagen α chains in basement membranes of human epidermis and skin appendages. *Arch. Histol. Cytol.* **2007**, *70*, 255–265. [CrossRef]
31. Vazquez, F.; Palacios, S.; Aleman, N.; Guerrero, F. Changes of the basement membrane and type IV collagen in human skin during aging. *Maturitas* **1996**, *25*, 209–215. [CrossRef]
32. Feru, J.; Delobbe, E.; Ramont, L.; Brassart, B.; Terryn, C.; Dupont-Deshorgue, A.; Garbar, C.; Monboisse, J.C.; Maquart, F.X.; Brassart-Pasco, S. Aging decreases collagen IV expression in vivo in the dermo-epidermal junction and in vitro in dermal fibroblasts: Possible involvement of TGF-beta1. *Eur. J. Dermatol.* **2016**, *26*, 350–360. [CrossRef]
33. Langton, A.K.; Halai, P.; Griffiths, C.E.; Sherratt, M.J.; Watson, R.E. The impact of intrinsic ageing on the protein composition of the dermal-epidermal junction. *Mech. Ageing Dev.* **2016**, *156*, 14–16. [CrossRef]
34. Aguirre-Cruz, G.; Leon-Lopez, A.; Cruz-Gomez, V.; Jimenez-Alvarado, R.; Aguirre-Alvarez, G. Collagen Hydrolysates for Skin Protection: Oral Administration and Topical Formulation. *Antioxidants* **2020**, *9*, 181. [CrossRef]
35. Hiramoto, K.; Sugiyama, D.; Takahashi, Y.; Mafune, E. The amelioration effect of tranexamic acid in wrinkles induced by skin dryness. *Biomed. Pharmacother.* **2016**, *80*, 16–22. [CrossRef]
36. Hiramoto, K.; Yamate, Y.; Sugiyama, D.; Matsuda, K.; Iizuka, Y.; Yamaguchi, T. Ameliorative effect of tranexamic acid on physiological skin aging and its sex difference in mice. *Arch. Dermatol. Res.* **2019**, *311*, 545–553. [CrossRef]
37. Hiramoto, K.; Yamate, Y.; Sugiyama, D.; Matsuda, K.; Iizuka, Y.; Yamaguchi, T. Effect of tranexamic acid in improving the lifespan of naturally aging mice. *Inflammopharmacology* **2019**, *27*, 1319–1323. [CrossRef]
38. Ogura, Y.; Matsunaga, Y.; Nishiyama, T.; Amano, S. Plasmin induces degradation and dysfunction of laminin 332 (laminin 5) and impaired assembly of basement membrane at the dermal-epidermal junction. *Br. J. Dermatol.* **2008**, *159*, 49–60. [CrossRef]
39. Endo, K.; Niki, Y.; Ohashi, Y.; Masaki, H. Tranexamic Acid Improves the Disrupted Formation of Collagen and Fibrillin-1 Fibers Produced by Fibroblasts Repetitively Irradiated with UVA. *Biol. Pharm. Bull.* **2021**, *44*, 225–231. [CrossRef]
40. Zhang, L.; Tan, W.Q.; Fang, Q.Q.; Zhao, W.Y.; Zhao, Q.M.; Gao, J.; Wang, X.W. Tranexamic Acid for Adults with Melasma: A Systematic Review and Meta-Analysis. *Biomed. Res. Int.* **2018**, *2018*, 1683414. [CrossRef]
41. Maeda, M.; Tomita, Y. Mechanism of the Inhibitory Effect of Tranexamic Acid on Melanogenesis in Cultured Human Melanocytes in the Presence of Keratinocyte-conditioned Medium. *J. Health Sci.* **2007**, *53*, 389–396. [CrossRef]
42. Voegeli, R.; Gierschendorf, J.; Summers, B.; Rawlings, A.V. Facial skin mapping: From single point bio-instrumental evaluation to continuous visualization of skin hydration, barrier function, skin surface pH, and sebum in different ethnic skin types. *Int. J. Cosmet. Sci.* **2019**, *41*, 411–424. [CrossRef]
43. Hashizume, H. Skin Aging and Dry Skin. *J. Dermatol.* **2004**, *31*, 603–609. [CrossRef]
44. Rovero, P.; Malgapo, D.M.H.; Sparavigna, A.; Beilin, G.; Wong, V.; Lao, M.P. The Clinical Evidence-Based Paradigm of Topical Anti-Aging Skincare Formulations Enriched with Bio-Active Peptide SA1-III (KP1) as Collagen Modulator: From Bench to Bedside. *Clin. Cosmet. Investig. Dermatol.* **2022**, *15*, 2693–2703. [CrossRef]
45. Amano, S. Characterization and mechanisms of photoageing-related changes in skin. Damages of basement membrane and dermal structures. *Exp. Dermatol.* **2016**, *25* (Suppl. S3), 14–19. [CrossRef]
46. Kobayashi, S.; Tsunematsu, N.; Morise, T.; Higashiura, C.; Yoshida, I.; Kuriyama, K. Why are Pigmented Spots Darker and Larger in Men? In Proceedings of the IFSCC Congress, Munich, Germany, 18–21 September 2018; IFSCC: New York, NY, USA, 2018.